EDGE ARTICLE

Check for updates

Constitutional adaptation to pK_a modulation by remote ester hydrolysis†

Ferran Esteve, [ID] * Tanguy Rieu [ID] and Jean-Marie Lehn [ID] *

The mechanisms through which environmental conditions affect the expression of interconnected species is a key step to comprehending the principles underlying complex chemical processes. In Nature, chemical modifications triggered by the environment have a major impact on the structure and function of biomolecules and regulate different reaction pathways. Yet, minimalistic artificial systems implementing related adaptation behaviours remain barely explored. The hydrolysis of amino acid methyl esters to their corresponding amino acids leads to a drastic change in pK_a (*ca.* 7 and 9, respectively) that protonates the free amino group at physiological conditions. Dynamic covalent libraries (DCvLs) based on amino acid methyl esters and aldehydes respond to such hydrolysis and lead to constitutional adaptation. Each of the libraries studied experiences a DCvL conversion allowing for constituent selection due to the silencing of the zwitterionic amino acids towards imine formation. The selective action of different enzymes on the DCvLs results in states with simplified constitutional distributions and transient chirality. When additional components (*i.e.*, scavengers) that are not affected by hydrolysis are introduced into the dynamic libraries, the amino acid methyl ester hydrolysis induces the up-regulation of the constituents made of these scavenging components. In these systems, the constituent distribution is resolved from a scrambled mixture of imines to a state characterized by the predominance of a single aldimine. Remarkably, although the final libraries display higher "simplexity", the different transient states present an increased complexity that allows for the emergence of organized structures [micelle formation] and distributions [up-regulation of two antagonistic constituents]. This reactive site inhibition by a remote chemical modification resembles the scenario found in some enzymes for the regulation of their activity through proximal post-translational modifications.

Introduction

Cross-talks between amino acid residues located at different positions in proteins control essential processes like molecular recognition and catalysis.[1] In addition, selective post-translational modifications (PTMs) on amino acid sidechains offer a powerful biological toolkit to expand the polypeptide functional repertoire.[2–4] These chemical modifications, occurring in well-defined microenvironments, commonly lead to large perturbations in the pK_a of surrounding ionizable groups that govern the function of biomolecules.[5] For instance, the phosphorylation of a serine residue induces changes in the pK_a of a nearby histidine sidechain and modulate the reactivity of cofilin proteins (Fig. 1A).[6] Therefore, chemical systems that can adapt to analogous remote transformations deserve to be

thoroughly explored as they might enlighten the mode-of-action underlying such biological processes.

An extensive amount of studies discussing adaptive systems rely on Constitutional Dynamic Chemistry (CDC) at either the molecular (Dynamic Covalent Chemistry, DCvC) or supramolecular level (Dynamic Non-Covalent Chemistry, DNCvC).[7] In DCvC, the reversible covalent bonds involved allow for error-checking and rearrangement processes under thermodynamic control.[8–11] Hence, the distribution of diversified Dynamic Covalent Libraries (DCvLs) can be directed to a certain state upon exposure to external stimuli or chemical effectors.[12,13] For example, the sorting of "messy" DCvLs has been attained using both physical (precipitation,[14] distillation,[15] adsorption[16]) and chemical (oxidation,[17] templates,[18] catalysis,[19] coupled enzymatic reactions[20]) methods. In a similar manner, Constitutional Dynamic Networks (CDNs) are composed of products (*i.e.*, constituents) constitutionally linked by exchangeable building blocks (*i.e.*, components) that adapt their distribution through agonistic and antagonistic relationships.[21,22] Substantial research efforts have been devoted to build-up relatively simple CDNs mimicking complex biological behaviours.[23–25] Related dynamic networks mediate the communication between

Laboratoire de Chimie Supramoléculaire, Institut de Science et d'Ingénierie Supramoléculaires (ISIS), Université de Strasbourg, 8 allée Gaspard Monge, 67000 Strasbourg, France. E-mail: estevefranch@unistra.fr; lehn@unistra.fr
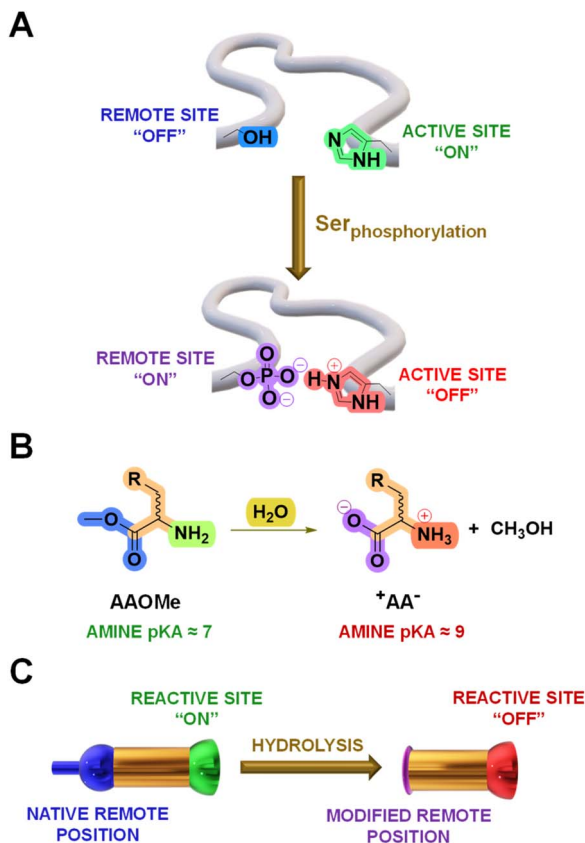
Fig. 1 (A) Representation of a decrease in activity at the catalytic site of a protein by a PTM (serine phosphorylation) accompanied by a change in the pK_a of a nearby residue (histidine protonation). (B) Hydrolysis of **AAOMe** (terminal −NH$_2$ site reactive in imination) to yield $^+$**AA**$^-$ (terminal −N$^+$H$_3$ site silent in imination) and a molecule of CH$_3$OH. (C) Representation of the proposed remote modification leading to the inhibition of the components of DCvLs (colour code has been maintained for comparison).

biomolecules (*e.g.*, DNA, RNA, proteins), leading to programmed reaction patterns that regulate key intracellular processes like signal transduction and enzymatic activity.[26] However, the design of DCvLs, and their underlying CDNs, able to undergo structural and/or constitutional adaptation in response to pK_a variations triggered by remote chemical modifications remains unexplored.

The hydrolysis of amino acid methyl esters (**AAOMe**) to their corresponding zwitterionic amino acids ($^+$**AA**$^-$) leads to a drastic pK_a change in the remote −NH$_2$ group, resulting in its protonation at neutral pH (predicted N$_\alpha$ pK_a values of *ca.* 9 and 7, respectively; Fig. 1B and Table S1†).[27] Thus, we envisaged that DCvLs based on the condensation of **AAOMe** and water-soluble aldehydes should experience constitutional adaptation in response to the hydrolysis of the remote ester group since the resulting zwitterionic $^+$**AA**$^-$ entity should be "poisoned" towards imine formation through reactive site protonation (Fig. 1C). After first devising the most reactive components towards imination, we optimized the conditions for the hydrolysis of the **AAOMe** ester group. Then, the time evolution of the DCvLs was investigated, observing that they resulted in states of higher "simplexity" (simplification of the

output of the system)[28] through transient states of higher complexity [enzymatic selection/transient chirality/sorting] and diversity [increased number of components/constituents]. Furthermore, such constituent selection induced emerging behaviours in the final simplified states of the libraries: micelle formation and antagonistic sorting (see below).

Results and discussion

Component screening

The first step was to select the reaction components by screening a series of water-soluble reactive aldehydes and different amines. Imines are generally disfavoured in water due to their propensity to hydrolyse back into the reactants.[29] Nevertheless, a rational design of the system (increased aldehyde electrophilicity and amine nucleophilicity) can assist to overcome this issue and foster relatively high yields.[30]

The imine yields for the reaction between different aldehydes, namely **A1–6**, and **ArgOMe** were evaluated at room temperature and pD = 7.0 (PBS 50 mM). ^{1}H NMR signal integration after 1 h of equilibration showed that the highest imine formation was observed when using **A1**, likely as a result of the strong electron-withdrawing capacity of the two sulfonate groups (Fig. 2A).

In terms of the amine screening, the studied α-**AAOMe** gave imine yields of *ca.* 30% (Fig. 2B). In contrast, the yield attained when using β-**AlaOMe** as a nucleophile was 9%, in good agreement with the higher pK_a calculated for this derivative (Table S1†). Several commercially available amines were also assayed to select a nucleophile with similar reactivity to that of the α-**AAOMe**. The most reactive amine was found to be **B1** which gave a remarkable imine yield of 67%, assigned to its low degree of protonation arising from the presence of a positive charge in close proximity.[31] A similar scenario was found in the case of **B2**, but with a lower imine formation (25% abundance). The amines presenting pK_a values between 8.7–9.3 (*viz.*, **B3**, **B5**, **B6**, and **B7**) resulted in imine yields of *ca.* 15%. As predicted, amine **B4** (pK_a = 10.2) did not react with aldehyde **A1** as its amino group is completely protonated at pD = 7.0. To increase the imine yields, the reaction between **A1** and **ArgOMe** was performed at higher concentrations maintaining a 1 : 1 ratio between components. The reaction at 80 mM gave 65% of imine **A1ArgOMe** (Fig. S1†). These results indicated that the low specificity of imine formation in water can be overcome at high concentrations and with adequate substrate selection, paving the way for the study of dynamic covalent reactions and libraries (see sections below).

Hydrolysis of AAOMe

Next, we decided to investigate the ester hydrolysis of **AAOMe**. It is well established that **AAOMe** are hydrolysed to the corresponding amino acids ($^+$**AA**$^-$) under basic conditions.[32] However, the pH must be optimized to attain the best conditions in terms of hydrolysis rates as well as imination efficiency and selection. Although higher pH values would favour imine formation and ester hydrolysis, undesired aldimines with $^+$**AA**$^-$ would also be formed at high pH (Table S2†). Thereby, three
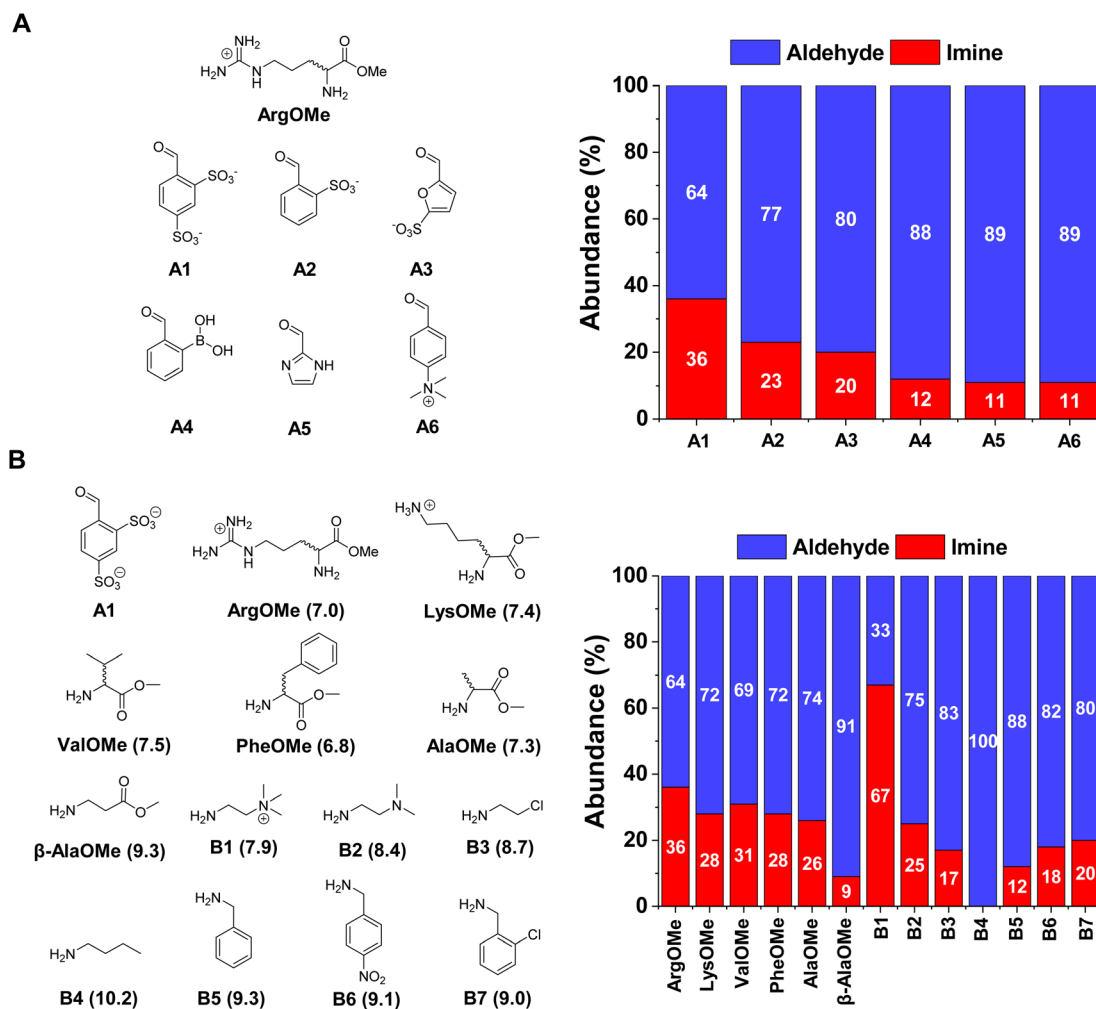
Fig. 2 (A) Aldehyde screening using **ArgOMe** as the model amine. (B) Amine screening using best-performing **A1** as aldehyde. Left: Chemical structures of the different reagents employed. Right: Component abundances obtained after equilibration (1 h at room temperature). The hydrate detected was included in the aldehyde composition. Amine pK_a values (calculated using MarvinSketch) have been included in brackets. All abundances were calculated using ^1H NMR spectroscopy (500 MHz, D_2O, pD = 7.0, PBS buffer 50 mM, 293 K). Initial concentration of reagents 5 mM each in all cases. Error in abundance: 5%.

experiments were run at pD values ranging from 6.2–7.8 to reveal the effect on the aforementioned variables.[33] The reaction course could be easily monitored by ^1H NMR spectroscopy, observing the disappearance of the signals assigned to **ArgOMe** and the appearance of those of $^+Arg^-$ and methanol (Fig. S2†). As expected, the fastest hydrolysis rates were obtained under basic conditions, with the reaction at pD = 7.8 being slightly favoured over the one at pD = 7.0 (Fig. S3 and Table S3†). Notwithstanding, the $-N_{\alpha/\beta}H_2$ degree of protonation calculated revealed that, at pD = 7.8, the $^+Arg^-$ inhibition towards imination would not be complete, as a significant amount of the reactive site would be in its nucleophilic non-protonated form (10%; see Table S2†). Separated reaction of **ArgOMe** and $^+Arg^-$ with **A1** at these different pD values corroborated this assumption (Table S4†). Although the highest imine yields were obtained at pD = 7.8 (44%), the undesired reaction between $^+Arg^-$ and **A1** was also detected (3% yield of **A1$^+$Arg$^-$**). On the other hand, slightly lower **A1ArgOMe** yields (36%) were noted at

pD = 7.0, but with complete silencing of **A1$^+$Arg$^-$** (entry 2, Table S4†). Therefore, the optimal pD was found to be 7.0.

We then evaluated the effect of the substrate structure on the hydrolysis rate, both in terms of the sidechain nature and the distance between the carbonyl unit and the amino group (*i.e.*, α- or β-**AAOMe**). Results suggest that β-**AAOMe** hydrolyses at slower rates than the α-derivatives. For instance, the hydrolysis of β-**AlaOMe** was much slower than that of **AlaOMe**, as shown by the yields of 16 and 44% observed after 48 h, respectively (Fig. S4 and Table S5†). In terms of the sidechain effect, the α-**AAOMe** presenting the highest hydropathy,[34] namely **ValOMe**, was barely hydrolysed after 48 h (≈ 20% CH_3OH yield; Fig. S4†). This could be related to a less efficient attack of water molecules on the ester group because of the hydrophobic environment. **LysOMe** presented the fastest hydrolysis rate, and the other α-**AAOMe** (*viz.* **ArgOME** and **PheOMe**) gave similar profiles (Table S5†). Thus, **LysOMe** was selected for the subsequent experiments (see sections below).

Previous reports proved that the hydrolysis of esters in water could be catalysed by imidazole-derivatives and by enzymes with esterase activity.[35,36] Acetylcholine esterase (**AChE**) is a conserved enzyme that presents superior activity in the hydrolysis of acetylcholine to choline (Fig. S5A†). The active site is composed of two well-defined functionalities: the esteratic site (containing a serine residue which cleaves the ester bonds) and the peripheral site (anionic groups that fix the substrate in the optimal position through supramolecular interactions).[37] We envisaged that **AChE** could selectively catalyse the hydrolysis of the **AAOMe** that contained a positively charged unit in the sidechain, namely **ArgOMe** and **LysOMe**, as they present a relatively similar chemical structure to that of acetylcholine (Fig. S5B†). The model hydrolysis of **ArgOMe** was then studied in the presence of imidazole and **AChE**. Whereas the imidazole-based approach was not successful even at high base concentrations (200 mol%), up to a 3.2-fold increase in hydrolysis rate could be observed with increasing catalytic amounts of **AChE** (Fig. S6 and Table S6†). As expected, the catalytic activity of **AChE** was notably dependent on the structure of the **AAOMe**, since it only accelerated the hydrolysis of **ArgOMe** and **LysOMe** (Fig. S7 and Table S7†). In view of these results, two additional **AAOMe** hydrolases were tested: **trypsin** and **chymotrypsin**. **Trypsin** was found to selectively catalyse the depletion of **LysOMe**, in a similar manner to that of **AChE**, but with faster rates (Fig. S8 and Table S8†). In contrast, **chymotrypsin** showed excellent selectivity for the catalytic hydrolysis of **PheOMe** (Fig. S8 and Table S8†).

Considering the chiral nature of the enzymatic active sites, we also surmised that **AChE** could preferentially catalyse the hydrolysis of one of the enantiomers of **LysOMe**. Indeed, the rate of hydrolysis of (**D**)**LysOMe** was not significantly affected by the enzyme (Fig. S9 and Table S9†). On the other hand, the use of 0.01 mol% of **AChE** induced complete hydrolysis of (**L**)**LysOMe** in less than 16 h.

Therefore, **AChE**, **trypsin** and **chymotrypsin** are suitable catalysts for the selective kinetic simplification of complex mixtures of **AAOMe** (*vide infra* **DCvL1**), as well as for challenging enantioselective kinetic resolutions of **AAOMe** racemic mixtures (*vide infra* **DCvL3**).

Constitutional adaptation to AAOMe hydrolysis in a dynamic covalent reaction

Several reports show how peptide-based supramolecular systems are able to assemble/disassemble in response to ester/anhydride hydrolysis, as a result of solubility differences between the generated carboxylate groups and the parent units.[38–41] However, the change in the reactivity of vicinal functionalities in response to such ester hydrolysis (*e.g.*, potential decrease in the nucleophilicity of surrounding groups by supramolecular cross-talks, see biological example in Fig. 1A) has been quite overlooked, as well as its implementation in dynamic covalent libraries.

Once the reaction conditions were optimized (see sections above), the effect of **AAOMe** hydrolysis on the imine yields was monitored for the reaction between **AAOMe** and **A1**. Considering that the $-N_{\alpha/\beta}H_2$ group of the hydrolysis product $^+AA^-$ is
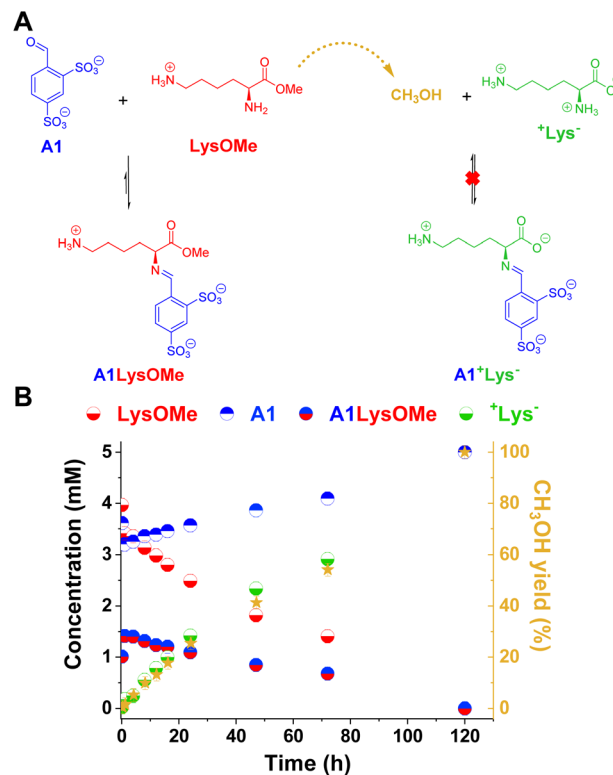

Fig. 3 (A) Chemical representation of the **LysOMe** reaction with **A1** influenced by the hydrolysis of **LysOMe** to produce $^+$**Lys**$^-$. (B) Concentration profile for the different species detected in solution over 120 h of reaction. The right Y-axis corresponds to the yield of methanol (dark yellow stars) calculated. Concentration and yields determined by ^{1}H NMR spectroscopy (500 MHz, D$_2$O, pD = 7.0, PBS buffer 50 mM, 293 K). The hydrate detected was included in the aldehyde concentration (mM). Initial concentration of reagents: 5 mM. Error bars correspond to 5% of the measurement.

protonated, this component should not react with the released aldehyde (see entry 2 in Table S4†), so that the final composition of the system is expected to consist predominantly of free **A1** and $^+$**AA**$^-$.

The reaction between **LysOMe** and **A1** (5 mM each) at room temperature in the absence of enzyme was monitored for 120 h using ^{1}H NMR spectroscopy (Fig. 3). The aldimine **A1LysOMe** was formed quite fast, reaching its maximum concentration of *ca.* 1.5 mM (30% yield) after 1 h of reaction. However, its concentration progressively decreased over time, as the hydrolysis of **LysOMe** occurred (see CH$_3$OH yield in Fig. 3B). As predicted, the final component distribution was $^+$**Lys**$^-$ (*ca.* 5 mM) and **A1** (*ca.* 5 mM), with aldimine **A1**$^+$**Lys**$^-$ not being detected. Subsequently, the adaptive response – and emergence of new properties – in more complex DCvLs was investigated (see following sections).

Dynamic covalent libraries (DCvLs)

Enzymatic action on 3-component [1 × 2] libraries. A competition experiment based on **A1** : **LysOMe** : **PheOMe** gave after 1 h a mixture of 2.9 mM **A1**, 4.1 mM **LysOMe**, and 3.8 mM **PheOMe**, together with 1.2 mM **A1LysOMe** and 0.7 mM **A1PheOMe** (**DCvL1**, Fig. 4A, B and S10†).
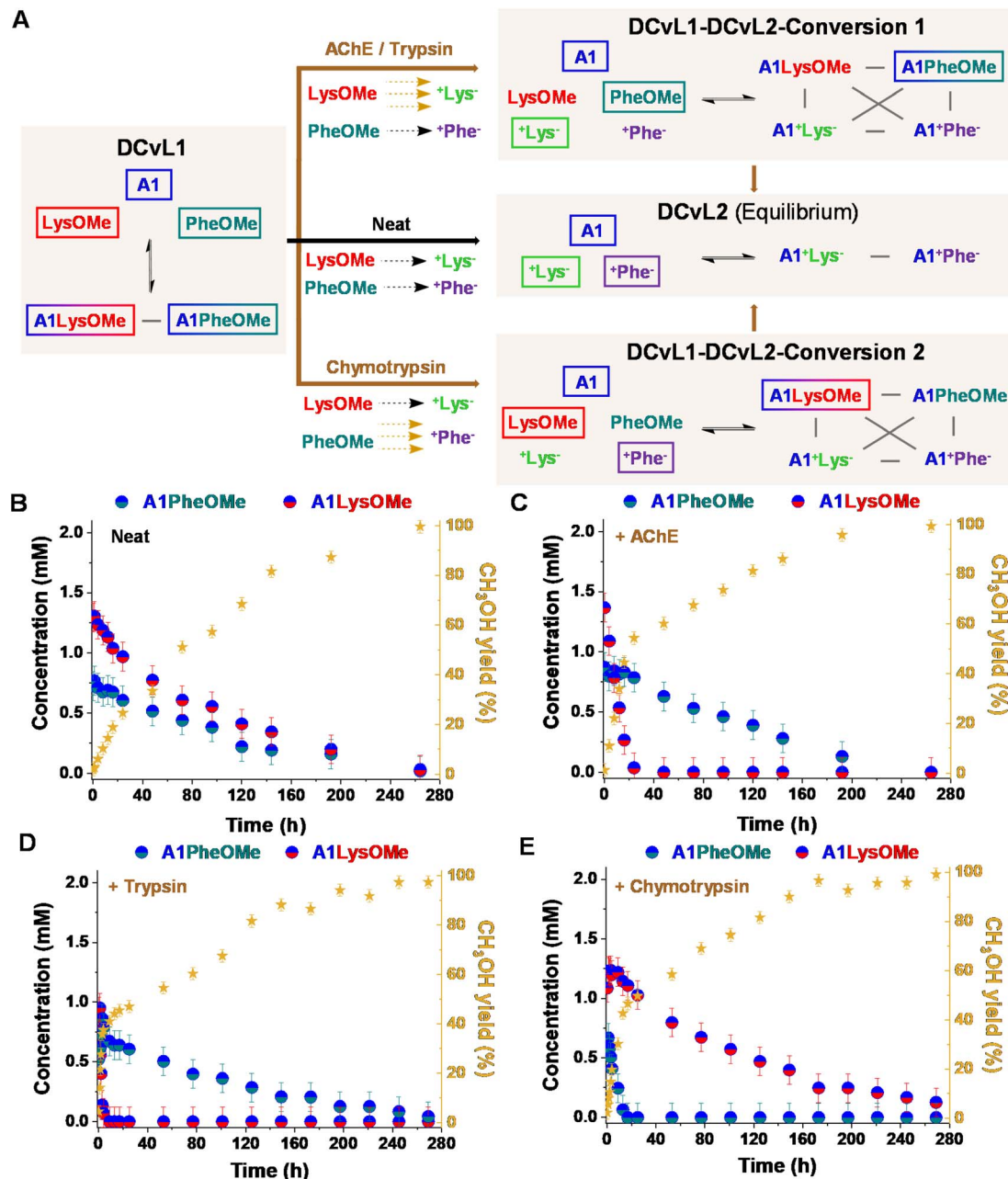
Fig. 4 (A) Reaction between **A1**, **LysOMe**, and **PheOMe** in the absence (black path) and presence of **AChE**, **trypsin** and **chymotrypsin** (brown paths, below). The **DCvL1-DCvL2-Conversion 1/2** (5 components, 4 constituents) from **DCvL1** (3 components, 2 constituents) to **DCvL2** (3 components, 2 constituents) have also been introduced. Predominant compounds (>0.7 mM) are marked with a coloured rectangle. Grey lines correspond to antagonistic relationships; the brown and black arrows represent the time evolution of **DCvL1** to reach **DCvL2**, in the presence and absence of enzymes, respectively. Concentration profile for the different constituents detected in solution over 264 h of reaction in the absence (B) and presence of (C) **AChE**, (D) **trypsin**, and (E) **chymotrypsin**. Concentration and yields determined by ^{1}H NMR spectroscopy (500 MHz, D$_2$O, pD = 7.0, PBS buffer 50 mM, 293 K). Initial concentration of reagents: 5 mM.

The hydrolysis of both **AAOMe** to their corresponding $^+$**AA**$^-$ derivatives converted **DCvL1** (3 components: **A1** : **LysOMe** : **PheOMe**, 2 constituents: **A1LysOMe** : **A1PheOMe**) into the **DCvL2** (3 components: **A1** : $^+$**Lys**$^-$: $^+$**Phe**$^-$, 2 constituents: **A1$^+$Lys$^-$** : **A1$^+$Phe$^-$**) through a transient state of higher constitutional complexity (5 components: **A1** : **LysOMe** : **PheOMe** : $^+$**Lys**$^-$: $^+$**Phe**$^-$, 4 constituents: **A1LysOMe** : **A1PheOMe** : $^+$**Lys**$^-$: $^+$**Phe**$^-$). After 264 h of reaction, the system reached the equilibrium characterized by

the absence of imines and the presence of **A1**, $^+$**Lys**$^-$, and $^+$**Phe**$^-$ (*ca.* 5 mM each, Fig. S10 and S11†). In the absence of an enzyme, a scrambled mixture of aldimines was always observed due to the subtly similar hydrolysis rates for **LysOMe** and **PheOMe**, with the concentration of constituent **A1LysOMe** being subtly higher than that of **A1PheOMe** (Fig. 4B and S4; see also Table S5†). However, when 0.01% of **AChE** was added to the mixture, a different scenario was found since this enzyme was able to selectively

catalyse the hydrolysis of **LysOMe** (Fig. S7 and Table S7†). **A1LysOMe** completely vanished within the first 24 h, because of the very efficient hydrolysis of **LysOMe** to $^+$**Lys**$^-$ catalysed by the enzyme. The concentration of these species after 20 h was of *ca.* 0.1 mM and 4.9 mM, respectively (Fig. S12 and S13†). Once the hydrolysis of **LysOMe** was completed, a drastic negative change in the slope CH_3OH yield was observed, accompanied by a minor up-regulation of **A1PheOMe** (Fig. 4C).[42] The fast and selective consumption of **LysOMe** resulted in a product distribution unattainable in the absence of enzyme, with **A1PheOMe** being the predominant aldimine constituent during the **DCvL1-DCvL2-Conversion 1**. **DCvL1** was also subjected to **trypsin** and **chymotrypsin** to study the distinct adaptive behaviour (*i.e.*, change in sorting selectivity) of this dynamic system. In the presence of **trypsin** (Fig. 4D), the new **DCvL1-DCvL2-Conversion 1** species distribution after 5 h was of **LysOMe** (<0.1 mM), **PheOMe** (3.8 mM), **A1LysOMe** (<0.1 mM), **A1PheOMe** (0.7 mM), $^+$**Lys**$^-$ (5 mM), and $^+$**Phe**$^-$ (0.4 mM), stressing that the only aldimine constituent during this higher-in-complexity state was **A1PheOMe** (Fig. S14†). Alternatively, **chymotrypsin** accelerated the hydrolysis of **PheOMe** (Fig. 4E), as evidenced by the predominance of the imine **A1LysOMe** (*ca.* 1 mM after 24 h) during the transient **DCvL1-DCvL2-Conversion 2** (Fig. 4A and E; see also Fig. S15†). With time, the imino-species that were not affected by the enzymes were also depleted, reaching in all cases the final **DCvL2** equilibrium state after *ca.* 264 h.

One notes that the lifetime of the sorted distribution might be modulated with the enzyme concentration. The **DCvL1** was thus studied in the presence of varying amounts of **chymotrypsin**. Whereas the use of 0.01% of the enzyme resulted in a transient sorting (**A1LysOMe** predominant aldimine) lasting for 250 h (Fig. S16B†), the introduction of 0.006 and 0.003% **chymotrypsin** resulted in sorted states for 240 h and 204 h, respectively (Fig. S16B and C†). Alternatively, when 0.03% of the enzyme was added, the **A1PheOMe** imine vanished in less than 4 h and the sorting was observed for 260 h (Fig. S16D†). These results inferred that the selectivity and lifetime of the sorted transient states can be easily controlled by the nature and the amount of enzyme introduced.

We also evaluated the possibility to build-up a similar library but based on a more challenging process: the selective chiral resolution of a racemic mixture induced by a remote modification. **AChE** was found to catalyse the hydrolysis of **(L)LysOMe** but it barely affected the hydrolysis rate of **(D)LysOMe** (Fig. S8 and Table S8†). The **DCvL3** using **A1** : **(L)LysOMe** : **(D)LysOMe** as components was then assayed (5 mM each, Fig. 5A). In this case, ^{1}H NMR analysis of the reaction course was less useful as it did not allow for differentiation between each pair of enantiomeric components, not even in the presence of water-soluble chiral shifting reagent [(R)-1,2-diaminopropane-N,N,N′,N′-tetraacetato]samarate(III).[43] Yet, one can estimate the abundance of each species considering the rates of hydrolysis for each separated
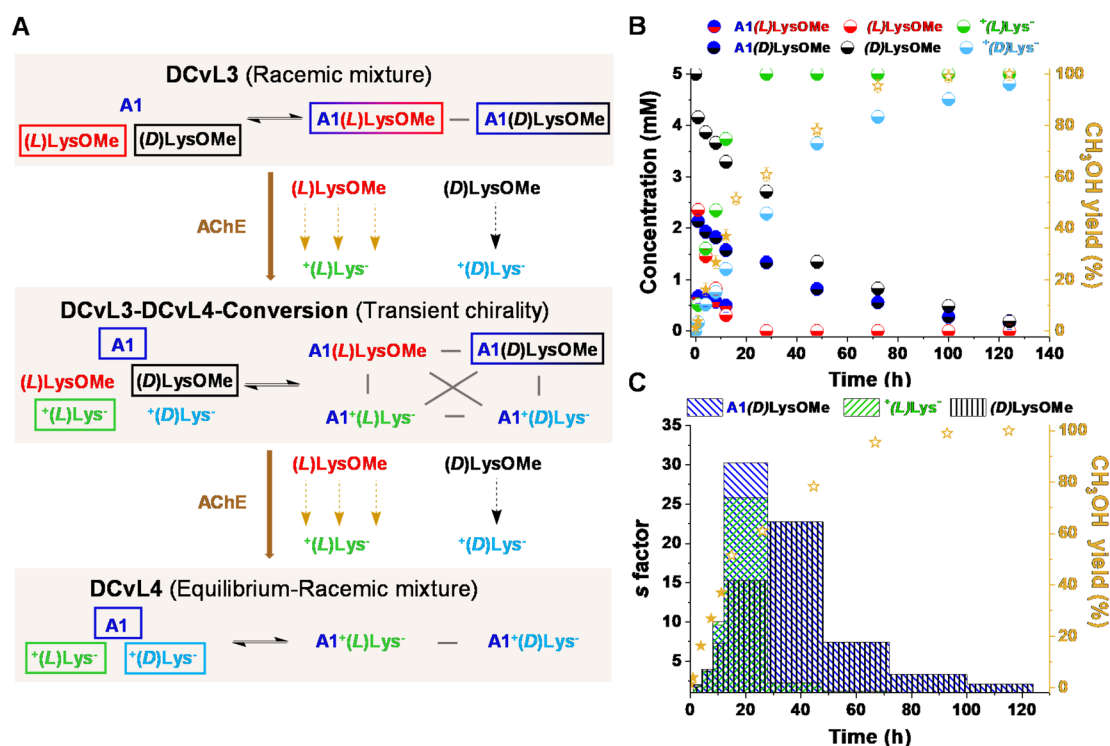

Fig. 5 (A) Reaction between **(D)LysOMe**, **(L)LysOMe** and **A1** in the presence of **AChE** (0.01 mol%). **DCvL3-DCvL4-Conversion** (5 components, 4 constituents) from **DCvL3** (3 components, 2 constituents) to **DCvL4** (3 components, 2 constituents) has also been introduced. Predominant compounds (>1.5 mM) are marked with a coloured rectangle. Grey lines correspond to antagonistic relationships; the brown arrows represent the time evolution of **DCvL3** to reach **DCvL4**. (B) Concentration profile for the different constituents detected in solution over 140 h. Concentration and yields determined by ^{1}H NMR spectroscopy (500 MHz, D_2O, pD = 7.0, PBS buffer 50 mM, 293 K). Initial concentration of reagents: 5 mM. (C) Time evolution of the *s* factors calculated for **A1(D)LysOMe**, $^+$**(L)Lys**$^-$, and **(D)LysOMe** over 126 h.

reaction and the yield of CH$_3$OH monitored for the kinetic resolution of the racemic mixture (see ESI† for more details). The time evolution for the different species revealed the conversion of the **DCvL3** to **DCvL4** (Fig. 5A). After 16 h of reaction, a severe deacceleration in CH$_3$OH production rate was observed, indicating that all (**L**)**LysOMe** had been consumed (Fig. S17†). At this point, the composition of the system was: (**L**)**LysOMe** (<0.1 mM), (**D**)**LysOMe** (2.5 mM), **A1**(**L**)**LysOMe** (<0.1 mM), **A1**(**D**)**LysOMe** (1.3 mM), $^+$(**L**)**Lys**$^-$ (5 mM), and $^+$(**D**)**Lys**$^-$ (2.1 mM) (Fig. 5B). Therefore, this higher-in-complexity **DCvL3-DCvL4-Conversion** (5 components, 4 constituents) presented remarkable transient chirality,[44] with the highest *s* factor of *ca.* 30 being attained after 24 h (Fig. 5C).[45,46] After 120 h, the complete consumption of both enantiomers of **LysOMe** was achieved, with the DCvL reaching its equilibrium state (**DCvL4**): a racemic mixture of $^+$(**L**)**Lys**$^-$ and $^+$(**D**)**Lys**$^-$ together with **A1** (5 mM each; Fig. S18†). These results emphasize how the selective action of different enzymes on DCvLs can drastically change their constitution, allowing for transient states of higher constitutional complexity with sorted distributions.

Chemically-driven selection in [1 × 2], [1 × 3] and [2 × 2] DCvLs

[1 × 2] DCvL. In the systems described above, the ester hydrolysis gave rise to the unreactive $^+$**AA**$^-$ component and the up-regulation of free aldehyde **A1**. It can be noted that if the competition experiments are performed in the presence of an amino component (**B2**) which can scavenge **A1**, the concentration of the resulting imine (**A1B2**) should be amplified with time as the silencing of the competing component **AAOMe** occurs by its conversion into $^+$**AA**$^-$. Initially, **DCvL5** (reaction between **A1**, **B2**, and **LysOMe**; Fig. 6A and S19A†) was studied at 5 mM concentration for each reagent. Nevertheless, only a minor increase in the concentration of **A1B2** was observed with time as the component **LysOMe** was hydrolysed to the inhibited $^+$**Lys**$^-$ (Fig. S19B and S20†). Based on previous results (Fig. S1†), we evaluated the **AAOMe** hydrolysis and imination reactions of **A1** and **AAOMe**/$^+$**AA**$^-$ at 80 mM. At such high concentrations, the kinetic profiles for the hydrolysis of **AAOMe** were comparable to the ones observed at 5 mM (Fig. S21 and Table S10 *vs.* Fig. S4 and Table S5†), but the reaction between $^+$**AA**$^-$ and **A1** could not be completely inhibited at 80 mM as some **A1**$^+$**AA**$^-$ aldimine was observed (*ca.* 5–10%, see Table S11†).

DCvL5 was then assessed at 80 mM to see the effect on both selection and activity. As expected, a more pronounced up-regulation of **A1B2** was noted, with a concentration increase of 17 mM after 400 h (Fig. 6B; see also Fig. S19B† for comparison). During the hydrolysis of **LysOMe**, the system experienced a conversion from **DCvL5** to **DCvL6**, with the corresponding increase in complexity during the **DCvL5-DCvL6-Conversion**: from 3 to 4 components and from 2 to 3 constituents (Fig. 6A).[28,47,48] The final composition of **DCvL6** was: 52 mM **A1B2**, 26 mM **A1**, 3 mM **A1**$^+$**Lys**$^-$, 77 mM $^+$**Lys**$^-$, and 28 mM **B2** (Fig. S22 and S23†). Remarkably, as the **LysOMe** hydrolysis occurred, the system evolved from a scrambled mixture of two constituents in **DCvL5** (*ca.* 35 mM of **A1B2** and **A1LysOMe**) to a sorted outcome in **DCvL6** containing **A1B2** as the main aldimine constituent.[49–51]
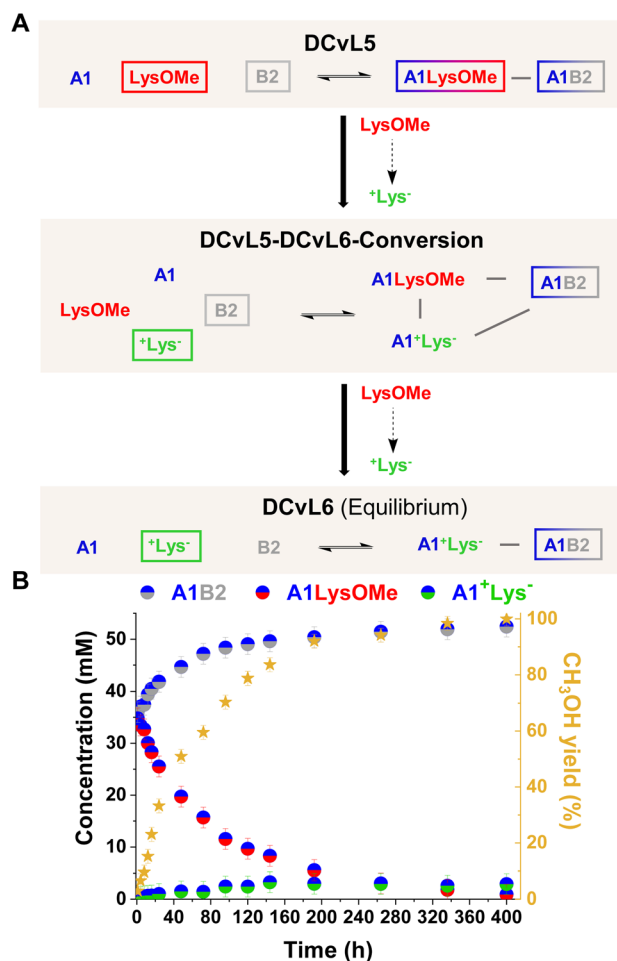

Fig. 6 (A) Reaction between **A1**, **LysOMe**, and **B2**. **DCvL5-DCvL6-Conversion** (5 components, 4 constituents) from **DCvL5** (3 components, 2 constituents) to **DCvL6** (3 components, 2 constituents) has also been represented. Predominant compounds (>35 mM) are marked with a coloured rectangle. Grey lines correspond to antagonistic relationships; the black arrows represent the time evolution of **DCvL5** to reach **DCvL6**. (B) Concentration profile for the different constituents detected in solution over 400 h of reaction. Concentration and yields determined by ^{1}H NMR spectroscopy (500 MHz, D$_2$O, pD = 7.0, PBS buffer 500 mM, 293 K). Initial concentration of reagents: 80 mM.

This chemically-driven adaptation in **DCvL5** was further studied in the absence of buffer (*i.e.* neat D$_2$O). The presence of the quite basic component **B2** led to an initial pD value of 8.3, resulting in slightly higher imine abundances than in the buffered system at pD 7.0 (*ca.* 40 mM and 35 mM, respectively; see Fig. 6B and S24†). The **LysOMe** to $^+$**Lys**$^-$ conversion triggered a similar constitutional rearrangement to that observed in the presence of buffer, but at subtly slower rates in this case. The equilibrium state of **DCvL6** was characterized by the absence of **A1LysOMe** and the predominance of **A1B2** (*ca.* 60 mM). During the **DCvL5-DCvL6-Conversion**, the pD of the system dropped 1.2 units as a result of the ester hydrolysis, reaching a final pD value of 7.1 (Fig. S25†). Thus, such noteworthy decrease in pD values regulated the expression of the **A1**$^+$**Lys**$^-$ constituent (in terms of imine formation) and allowed for a sorted state with higher fidelity in **DCvL6**.
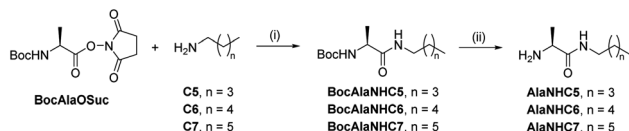
Scheme 1 Two-step synthesis of amphiphilic pseudopeptidic compounds AlaNHCX. (i) DCM, r.t., 16 h. (ii) TFA, DCM, r.t., 3 h.

[1 × 3] DCvL. We decided to study the behaviour of related [1 × 3] systems on addition of a further adaptive step by combining the up-regulation of the unaffected constituent to the generation of a macroscopic property. To this end, a new family of amphiphilic pseudopeptidic compounds with different chain lengths (**AlaNHCX**, Scheme 1) was synthesized following reported procedures.[52] These amines were selected since their aldimine derivatives formed upon reaction with a charged aldehyde (*e.g.*, **A1**) should present a prominent tendency to self-assemble in water and form micelles.[53] ^{1}H NMR at 80 mM indicated yields of *ca.* 50% for the imines **A1AlaNHCX** (see Table S12†). These values, despite being slightly lower than those of **AAOMe** under the same conditions, showed that the pseudopeptides were suitable for competition experiments. Moreover, the concentration of the aldimines **A1AlaNHCX** was not altered over time, indicating that the amide bond was stable to hydrolysis for at least 1 month.

The self-assembling properties of the different compounds were then evaluated by fluorescence emission spectroscopy using nile red (NR) as a hydrophobic probe.[54] SDS was used as a control for the fluorescence emission values of a system containing micelles. The parent amines **AlaNHCX** barely formed micelles even at high concentrations (80 mM, Fig. S26†). In contrast, aldimine derivatives were found active in micellization. For instance, **A1AlaNHC7** seemed to self-assemble into micellar structures, as evidenced by the intense fluorescence response observed (Fig. S27†). The CMC for **A1AlaNHC7** was in the 7–12 mM range. DLS analyses of the **A1AlaNHC7** sample at 12 mM revealed the presence of micelles with an average diameter of 7.9 nm (Fig. S28†).

The hydrolysis reactions occurring in the **DCvL7** (**A1**, **LysOMe**, **ArgOMe** and **AlaNHC7**; 1 eq. each) should result in the decrease of **A1LysOMe** and **A1ArgOMe** together with an up-regulation of **A1AlaNHC7** over time (Fig. 7A). When the concentration of **A1AlaNHC7** increases from below to above CMC, the spontaneous formation of micelles (**A1AlaNHC7-mic**) should be noted in the solution. Reaction between **A1** : **LysOMe** : **ArgOMe** : **AlaNHC7** (35 mM each) resulted in the **DCvL7** with a constituent concentration of 10, 9, and 6 mM respectively for **A1LysOMe**, **A1ArgOMe**, and **A1AlaNHC7**. Since the concentration of **A1AlaNHC7** was below the CMC, the relative fluorescence response observed was of 0.3, in good agreement with the absence of micelles.

The hydrolysis of **ArgOMe** and **LysOMe** to their corresponding $^+$**AA**$^-$ released **A1** into the medium, as the hydrolysed amino acids were silent towards imination due to protonation. **AlaNHC7** scavenged the generated aldehyde and led to an amplification of **A1AlaNHC7**. After 90 h of reaction, the
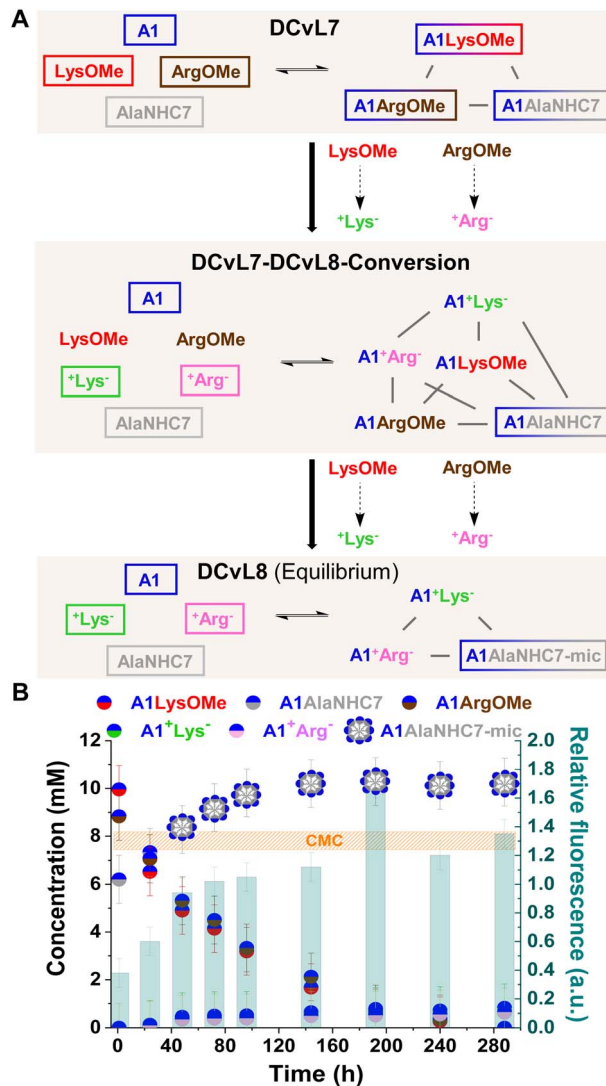

Fig. 7 (A) Reaction between A1, LysOMe, ArgOMe, and AlaNHC7. DCvL7-DCvL8-Conversion (6 components, 5 constituents) from DCvL7 (4 components, 3 constituents) to DCvL8 (4 components, 3 constituents) has also been represented. Predominant compounds (>5 mM) are marked with a coloured rectangle. Grey lines correspond to antagonistic relationships; the black arrows represent the time evolution of DCvL7 to reach DCvL8. (B) Concentration profile for the different constituents detected in solution over 290 h of reaction. Concentrations determined by ^{1}H NMR spectroscopy (500 MHz, D$_2$O, pD = 7.0, PBS buffer 500 mM, 293 K). Initial concentration of reagents: 35 mM. CMC determined by fluorescence spectroscopy.

concentration of **A1AlaNHC7** was of *ca.* 10 mM, with a relative fluorescence emission >1 (Fig. 7B). Therefore, **A1AlaNHC7** assemblies (namely **A1AlaNHC7-mic**) were present in the solution. Such high relative fluorescence values were maintained over time, indicating that the micelles were stable under the conditions assayed. DLS analyses for the final sample revealed the presence of micelles with a hydrodynamic diameter of 7.2 nm. The observed **DCvL7-DCvL8-Conversion** presented a higher complexity (6 components, 5 constituents) than the initial and final states (**DCvL7** and **DCvL8**, respectively, both with 4 components and 3 constituents). The equilibrium

distribution of the **DCvL8** was of 10 mM **A1AlaNHC7-mic**, 1 mM **A1$^+$Lys$^-$**, 1 mM **A1$^+$Arg$^-$**, 25 mM **A1**, 34 mM **$^+$Lys$^-$** and 34 mM **$^+$Arg$^-$** (Fig. S29 and S30†). Therefore, **DCvL7** experiences a triple-state adaptation: DCvL conversion + selective constituent amplification + formation of self-assembled dynamic micelles; resulting in the emergence of a property neither contained in the components nor in the initial library.

[2 × 2] DCvL. Finally, the adaptive behaviour of a [2 × 2] DCvL was also studied. As reported, [2 × 2] CDNs respond to constitutional relationships between species upon addition of

certain effectors.[55–57] The up-regulation of the most thermodynamically-favoured constituent of a network (*e.g.*, AB) is accompanied by the amplification of its agonistic – and least fitted – A′B′ constituent, at expenses of the antagonistic AB′ and A′B constituents.[7,26] We surmised that building-up a [2 × 2] library in which one of the competing amines is silenced by hydrolysis should result in a simultaneous increase in concentration of the two antagonistic constituents that are not hydrolysed.

The initial distribution of **DCvL9**, built-up from **LysOMe**, **B2**, **A1** and **A3** (Fig. 8A), revealed that the aldimines derived from **A1** were present in higher concentrations (*ca.* 35 mM) than those of **A3** (*ca.* 20 mM) as a result of its higher reactivity (see Fig. 2A and B). As the **LysOMe** ester hydrolysis proceeded, **DCvL9** converted into **DCvL10** through the higher-in-complexity **DCvL9-DCvL10-Conversion**, as seen from the ^{1}H NMR spectra by the appearance of **$^+$Lys$^-$** signals. This hydrolysed component barely reacted with the aldehydes, resulting in the up-regulation of **A1B2** and **A3B2**. Despite their antagonistic relationship -both constituents contain **B2** as building block-, an increase in concentration of *ca.* 15 and 10 mM was noted for **A1B2** and **A3B2**, respectively (Fig. 8B). The species distribution after 264 h of reaction was: 50 mM **A1B2**, 28 mM **A3B2**, 3 mM **A1$^+$Lys$^-$**, < 1 mM **A3$^+$Lys$^-$**, 29 mM **A1**, 48 mM **A3**, 77 mM **$^+$Lys$^-$** and 2 mM **B2** (Fig. S31 and S32†). Thus, the DCvL conversion, triggered by ester hydrolysis, led to the constitutionally-disfavoured up-regulation of two antagonistic constituents in **DCvL10** (see Fig. 8A). This behaviour resulted from the high degree of protonation of the competing amine (*i.e.*, **$^+$Lys$^-$**) that stimulated the scavenging of **A1** and **A3** by **B2**.

Conclusions

The hydrolysis of different **AAOMe** constituents to their corresponding **$^+$AA$^-$** in a series of **DCvLs** affects imine formation with several aldehydes. This remote chemical modification increases the protonation degree of the N$_{\alpha/\beta}$ amino group due to the lower pK_a of the hydrolysed species, thus hampering imine formation.

Monitoring the reaction between **LysOMe** and **A1** showed the expected depletion of **A1LysOMe** as **$^+$Lys$^-$** was produced, with the aldimine **A1$^+$Lys$^-$** not being observed due to the protonation of **$^+$Lys$^-$** (inhibited component). The kinetic simplification of two dynamic libraries (**DCvL1** and **DCvL3**) in the presence of different enzymes (*i.e.*, **AChE**, **trypsin** and **chymotrypsin**) was attained, with the catalysed remote chemical modification leading to selective silencing of components, sorted states and transient chirality. In [1 × 2] and [1 × 3] DCvLs, containing a component that was not hydrolysed (*i.e.*, the scavenger **B2** or **AlaNHC7**), the hydrolysis of the **AAOMe** resulted in the up-regulation of the constituents made of these components. Such DCvLs experienced a chemically-driven constitutional sorting, evolving from an almost statistical distribution (2 and 3 aldimines for **DCvL5** and **DCvL7**, respectively) to a state characterized by the predominance of a single imine. In addition, the **DCvL7** displayed a triple-state adaptation based on DCvL conversion, selective constituent up-regulation and supramolecular self-assembly with emergence of a macroscopic property
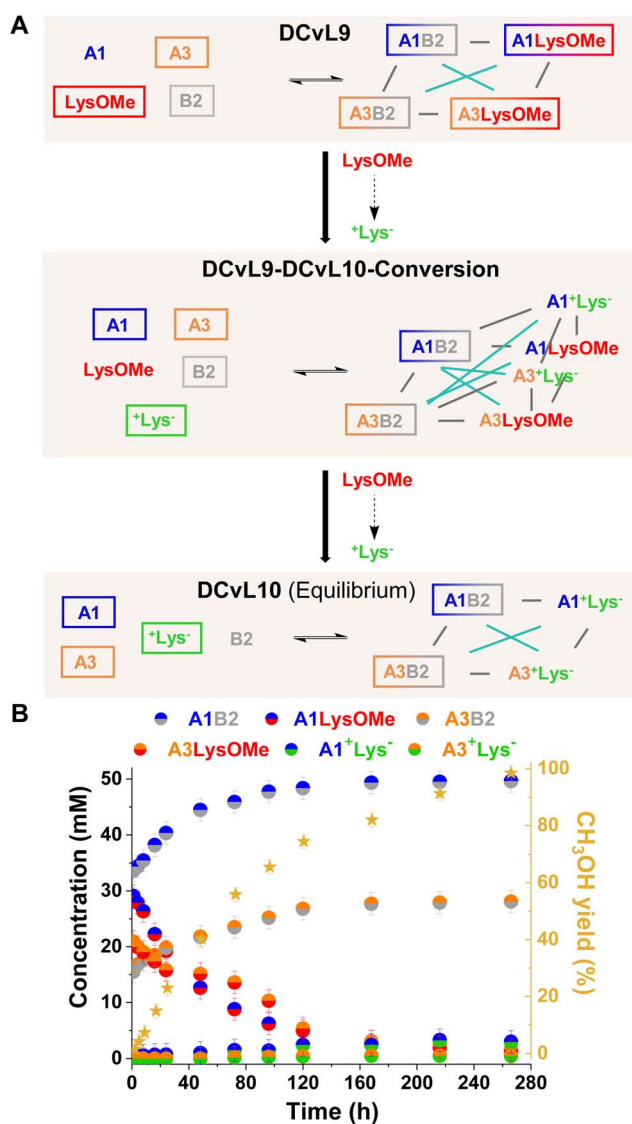

Fig. 8 (A) Reaction between A1, A3, LysOMe, and B2. DCvL9-DCvL10-Conversion (5 components, 6 constituents) from DCvL9 (4 components, 4 constituents) to DCvL10 (4 components, 4 constituents) has also been represented. Predominant compounds (>15 mM) are marked with a coloured rectangle. Grey and cyan lines correspond to antagonistic and agonistic relationships, respectively; the black arrows represent the time evolution of DCvL9 to reach DCvL10. (B) Concentration profile for the different constituents detected in solution over 264 h of reaction. Concentration and yields determined by ^{1}H NMR spectroscopy (500 MHz, D$_2$O, pD = 7.0, PBS buffer 500 mM, 293 K). Initial concentration of reagents: 80 mM.

that was not present in the initial library: the generation of micelles. A $[2 \times 2]$ library was also constructed in which one of the amino components was selectively poisoned by hydrolysis. The conversion from **DCvL9** to **DCvL10** resulted in a concentration increase for two constituents with an antagonistic relationship. Thus, all the DCvLs studied present transient states of higher constitutional complexity that adapt and evolve with time to states of higher "simplexity". In addition, the interplay between the action of different enzymes and the libraries dictates the selectivity and the lifetime of the transient sorted states (up-regulated constituent and/or chirality).

In a broader sense, such adaptive responses in simple dynamic networks offer an evolutionarily relevant scenario were a remote side-reaction triggered by the environment (*i.e.*, solvent) amplifies the population of the "surviving" constituents at the expense of the "poisoned" ones which undergo the detrimental chemical modification. These results will pave the way for the design of related dynamic systems of higher functionality with emerging functions. Furthermore, the observed silencing process based on reactive site protonation showcases the mode-of-action found in some proteins for the regulation of their activity through specific PTMs that lead to pK_a modulations. Therefore, this work will also contribute to our knowledge on sophisticated biological mechanisms governed by supramolecular cross-talks between remote sites.

Data availability

Data available upon request from the authors.

Author contributions

The manuscript was written through contributions of all authors. All authors have given approval to the final version of the manuscript. Conceptualization: F. E., J. M. L. Data curation: F. E., T. R. Formal analysis: F. E. Funding acquisition: J. M. L. Investigation: T. R. (supporting), F. E. (lead). Methodology: F. E. Project administration: J. M. L. Resources: J. M. L. Supervision: F. E., J. M. L. Validation: F. E. Visualization: F. E. Writing original draft: F. E. Writing – review and editing: T. R. (supporting), F. E., J. M. L.

Conflicts of interest

There are no conflicts to declare.

Acknowledgements

Notes and references

1 W. P. Jencks, *Catalysis in Chemistry and Enzymology*, McGraw-Hill, New York, 1969.

2 V. Csizmok and J. D. Forman-Kay, Complex regulatory mechanisms mediated by the interplay of multiple post-translational modifications, *Curr. Opin. Struct. Biol.*, 2018, **48**, 58–67.

3 Z. A. Wang and P. A. Cole, The Chemical Biology of Reversible Lysine Post-translational Modifications, *Cell Chem. Biol.*, 2020, **27**, 953–969.

4 A. V. Probst, E. Dunleavy and G. Almouzni, Epigenetic inheritance during the cell cycle, *Nat. Rev. Mol. Cell Biol.*, 2009, **10**, 192–206.

5 D. G. Isom, C. A. Castañeda, B. R. Cannon and B. García-Moreno, Large shifts in pKa values of lysine residues buried inside a protein, *Proc. Natl. Acad. Sci. U. S. A.*, 2011, **108**, 5260–5265.

6 A. Schonichen, B. A. Webb, M. P. Jacobson and D. L. Barber, Considering Protonation as a Post-translational Modification Regulating Protein Structure and Function, *Annu. Rev. Biophys.*, 2013, **42**, 289–314.

7 J.-M. Lehn, Constitutional Dynamic Chemistry, *Top. Curr. Chem.*, 2012, **322**, 1–32.

8 J.-M. Lehn, Perspectives in Chemistry-Steps towards Complex Matter, *Angew. Chem., Int. Ed.*, 2013, **52**, 2836–2850.

9 S. P. Black, J. K. M. Sanders and A. R. Stefankiewicz, Disulfide exchange: exposing supramolecular reactivity through dynamic covalent chemistry, *Chem. Soc. Rev.*, 2014, **43**, 1861–1872.

10 K. Acharyya and P. S. Mukherjee, Organic Imine Cages: Molecular Marriage and Applications, *Angew. Chem., Int. Ed.*, 2019, **58**, 8640–8653.

11 B. T. Herrera, S. R. Moor, M. McVeigh, E. K. Roesner, F. Marini and E. V. Anslyn, Rapid Optical Determination of Enantiomeric Excess, Diastereomeric Excess, and Total Concentration Using Dynamic-Covalent Assemblies: A Demonstration Using 2-Aminocyclohexanol and Chemometrics, *J. Am. Chem. Soc.*, 2019, **141**, 11151–11160.

12 A. Chevalier, A. Osypenko, J.-M. Lehn and D. Meyer, Phase transfer of metal cations by induced dynamic carrier agents: biphasic extraction based on dynamic covalent chemistry, *Chem. Sci.*, 2020, **11**, 11468–11477.

13 B. Liu, M. A. Beatty, C. G. Pappas, K. Liu, J. Ottelé and S. Otto, Self-Sorting in Dynamic Combinatorial Libraries Leads to the Co-Existence of Foldamers and Self-Replicators, *Angew. Chem., Int. Ed.*, 2021, **60**, 13569–13573.

14 R. C. Lirag, K. Osowska and O. S. Miljanic, Precipitation-driven self-sorting of imines, *Org. Biomol. Chem.*, 2012, **10**, 4847–4850.

15 K. Osowska and O. S. Miljanic, Self-sorting of dynamic imine libraries during distillation, *Angew. Chem., Int. Ed.*, 2011, **50**, 8345–8349.

16 C.-W. Hsu and O. S. Miljanic, Adsorption-driven self-sorting of dynamic imine libraries, *Angew. Chem., Int. Ed.*, 2015, **54**, 2219–2222.

17 K. Osowska and O. S. Miljanic, Oxidative kinetic self-sorting of a dynamic imine library, *J. Am. Chem. Soc.*, 2011, **133**, 724–727.

18 S. Gambaro, C. Talotta, P. Della Sala, A. Soriente, M. De Rosa, C. Gaeta and P. Neri, Kinetic and Thermodynamic Modulation of Dynamic Imine Libraries Driven by the Hexameric Resorcinarene Capsule, *J. Am. Chem. Soc.*, 2020, **142**, 14914–14923.

19 F. Schaufelberger and O. Ramström, Kinetic Self-Sorting of Dynamic Covalent Catalysts with Systemic Feedback Regulation, *J. Am. Chem. Soc.*, 2016, **138**, 7836–7839.

20 P. Vongvilai, M. Angelin, R. Larsson and O. Ramström, Dynamic Combinatorial Resolution: Direct Asymmetric Lipase-Mediated Screening of a Dynamic Nitroaldol Library, *Angew. Chem., Int. Ed.*, 2007, **46**, 948–950.

21 G. Men and J.-M. Lehn, Multiple adaptation of constitutional dynamic networks and information storage in constitutional distributions of acylhydrazones, *Chem. Sci.*, 2019, **10**, 90–98.

22 S. Wang, L. Yue and I. Willner, Enzyme-Guided Selection and Cascaded Emergence of Nanostructured Constitutional Dynamic Networks, *Nano Lett.*, 2020, **20**, 5451–5457.

23 C. Wang, L. Yue and I. Willner, Controlling biocatalytic cascades with enzyme–DNA dynamic networks, *Nat. Catal.*, 2020, **3**, 941–950.

24 C. Wang, M. P. O'Hagan, E. Neumann, R. Nechushtai and I. Willner, Integration of photocatalytic and dark-operating catalytic biomimetic transformations through DNA-based constitutional dynamic networks, *Nat. Commun.*, 2021, **12**, 4224.

25 Y. Ouyang, P. Zhang and I. Willner, Dynamic Catalysis Guided by Nucleic Acid Networks and DNA Nanostructures, *Bioconjugate Chem.*, 2023, **34**, 51–69.

26 L. Yue, S. Wang, Z. Zhou and I. Willner, Nucleic Acid Based Constitutional Dynamic Networks: From Basic Principles to Applications, *J. Am. Chem. Soc.*, 2020, **142**, 21577–21594.

27 Calculated using MarvinSketch; see Table S1† for predicted pK_a values and –N$_{\alpha/\beta}$H$_2$ protonation degree (%) of **AAOMe** and **$^+$AA$^-$**.

28 A. Osypenko, R. Cabot, J. J. Armao IV, P. Kovaricek, A. Santoro and J.-M. Lehn, Behavior of Constitutional Dynamic Networks: Competition, Selection, Self-sorting in Cryptate Systems, *ChemistryEurope*, 2023, **1**, e202300017.

29 M. S. Li, Y. W. Dong, M. Quan and W. Jiang, Stabilization of Imines and Hemiaminals in Water by an Endo-Functionalized Container Molecule, *Angew. Chem., Int. Ed.*, 2022, **61**, e202208508.

30 C. Godoy-Alcántar, A. K. Yatsimirsky and J.-M. Lehn, Structure-Stability Correlations for Imine Formation in Aqueous Solution, *J. Phys. Org. Chem.*, 2005, **18**, 979–985.

31 A. Bencini, A. Bianchi, E. García-España, M. Micheloni and J. A. Ramirez, Proton coordination by polyamine compounds in aqueous solution, *Coord. Chem. Rev.*, 1999, **188**, 97–156.

32 P. A. Khalaf-Alla, M. M. Shoukry, A. A. Jbarah and R. van Eldik, Base hydrolysis of α-amino acid esters catalysed by [Pd(N-ethylethylenediamine)(H$_2$O)$_2$]$^{2+}$. Kinetic study and DFT calculations, *Inorg. Chim. Acta*, 2017, **458**, 181–189.

33 Considering that pH = pD + 0.4, the pH values monitored were: 6.6, 7.4, and 8.2. These are the values at which the –N$_{\alpha/\beta}$H$_2$ degree of protonation was calculated (Table S2†).

34 J. Kyte and R. F. Doolittle, A simple method for displaying the hydropathic character of a protein, *J. Mol. Biol.*, 1982, **157**, 105–132.

35 M. Tanihara and Y. Imanishi, Highly Efficient and Enantiomer-Selective Hydrolysis of α-Amino Acid Active Ester Hydrochlorides by a Cyclic Hexapeptide Containing Histidines, *Polym. J.*, 1983, **15**, 499–507.

36 T. Takahashi, Y. Yamazaki and K. Kato, Substrate Specificity of an a-Amino Acid Ester Hydrolase Produced by Acetobacter turbidans A.T.C.C. 9325, *Biochem. J.*, 1974, **137**, 497–503.

37 T. Bunyapaiboonsri, O. Ramström, S. Lohmann, J.-M. Lehn and M. Goeldner, Dynamic Deconvolution of a Pre-Equilibrated Dynamic Combinatorial Library of Acetylcholinesterase Inhibitors, *ChemBioChem*, 2001, **2**, 438–444.

38 J. Boekhoven, W. E. Hendriksen, G. J. M. Koper, R. Eelkema and J. H. Van Esch, Transient assembly of active materials fueled by a chemical reaction, *Science*, 2015, **349**, 1075–1079.

39 M. Tena-Solsona, B. Rieb, R. K. Grötsch, F. C. Löhrer, C. Wanzke, B. Käsdorf, A. R. Bausch, P. Müller-Buschbaum, O. Lieleg and J. Boekhoven, Non-equilibrium dissipative supramolecular materials with a tunable lifetime, *Nat. Commun.*, 2017, **8**, 15895.

40 B. Rieb, C. Wanzke, M. Tena-Solsona, R. K. Grötsch, C. Maity and J. Boekhoven, Dissipative assemblies that inhibit their deactivation, *Soft Matter*, 2018, **14**, 4852–4859.

41 A. M. Bergmann, J. Bauermann, G. Bartolucci, C. Donau, M. Stasi, L. Holtmannspötter, F. Jülicher, C. A. Weber and J. Boekhoven, Liquid spherical shells are a non-equilibrium steady state of active droplets, *Nat. Commun.*, 2023, **14**, 6552.

42 In a system where the imine reactions do not have such low yields, the up-regulation will be more pronounced.

43 A. Inamoto, K. Ogasawara, K. Omata, K. Kabuto and Y. Sasaki, Samarium(III)-propylenediaminetetraacetate complex: A water-soluble chiral shift reagent for use in high-field NMR, *Org. Lett.*, 2000, **23**, 3543–3545.

44 Y. Sakata, S. Chiba and S. Akine, Transient chirality inversion during racemization of a helical cobalt(III) complex, *Proc. Natl. Acad. Sci. U. S. A.*, 2022, **119**, e2113237119.

45 A. Kamal, M. A. Azhar, T. Krishnaji, M. S. Malik and S. Azeeza, Approaches based on enzyme mediated kinetic to dynamic kinetic resolutions: A versatile route for chiral intermediates, *Coord. Chem. Rev.*, 2008, **252**, 569–592.

46 M. D. Greenhalgh, J. E. Taylor and A. W. Smith, Best practice considerations for using the selectivity factor, s, as a metric for the efficiency of kinetic resolutions, *Tetrahedron*, 2018, **74**, 5554–5560.

47 P. Kovaricek, A. C. Meister, K. Flidrova, R. Cabot, K. Kovarickova and J.-M. Lehn, Competition-driven selection in covalent dynamic networks and
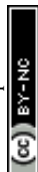
implementation in organic reactional selectivity, *Chem. Sci.*, 2016, **7**, 3215–3226.

48 Z. Yang, F. Esteve, C. Antheaume and J.-M. Lehn, Dynamic covalent self-assembly and self-sorting processes in the formation of imine-based macrocycles and macrobicyclic cages, *Chem. Sci.*, 2023, **14**, 6631–6642.

49 P. Howlader and P. S. Mukherjee, Face and edge directed self-assembly of Pd12 tetrahedral nano-cages and their self-sorting, *Chem. Sci.*, 2016, **7**, 5893–5899.

50 V. Abet, F. T. Szczypinski, M. A. Little, V. Santolini, C. D. Jones, R. Evans, C. Wilson, X. Wu, M. F. Thorne, M. J. Bennison, P. Cui, A. I. Cooper, K. E and A. G. Slater, Inducing Social Self-Sorting in Organic Cages To Tune The Shape of The Internal Cavity, *Angew. Chem., Int. Ed.*, 2020, **59**, 16755–16763.

51 A. Kumar and P. S. Mukherjee, Multicomponent Self-Assembly of Pd^{II}/Pt^{II} Interlocked Molecular Cages: Cage-to-Cage Conversion and Self-Sorting in Aqueous Medium, *Chem.–Eur. J.*, 2020, **26**, 4842–4849.

52 M. Allan, S. Manku, E. Therrien, N. Nguyen, S. Styhler, M.-F. Robert, A.-C. Goulet, A. J. Petschner, G. Rahil, A. R. MacLeod, R. Déziel, J. M. Besterman, H. Nguyen and A. Wahhab, *N*-Benzyl-1-heteroaryl-3-(trifluoromethyl)-1*H*-pyrazole-5-carboxamides as inhibitors of co-activator associated arginine methyltransferase 1 (CARM1), *Bioorg. Med. Chem. Lett.*, 2009, **19**, 1218–1223.

53 C. B. Minkenberg, L. Florusee, R. Eelkema, G. J. M. Koper and J. H. van Esch, Triggered Self-Assembly of Simple Dynamic Covalent Surfactants, *J. Am. Chem. Soc.*, 2009, **131**, 11274–11275.

54 M. C. A. Stuart, J. C. van de Pas and J. B. F. N. Engberts, The use of Nile Red to monitor the aggregation behavior in ternary surfactant–water–organic solvent systems, *J. Phys. Org. Chem.*, 2005, **18**, 929–934.

55 M. He and J.-M. Lehn, Time-dependent switching of constitutional dynamic libraries and networks from kinetic to thermodynamic distributions, *J. Am. Chem. Soc.*, 2019, **141**, 18560–18569.

56 J.-F. Ayme, S. Dhers and J.-M. Lehn, Triple Self-Sorting in Constitutional Dynamic Networks: Parallel Generation of Imine-Based CuI, FeII, and ZnII Complexes, *Angew. Chem., Int. Ed.*, 2020, **59**, 12484–12492.

57 J.-F. Ayme and J.-M. Lehn, Self-sorting of two imine-based metal complexes: balancing kinetics and thermodynamics in constitutional dynamic networks, *Chem. Sci.*, 2020, **11**, 1114–1121.